Article

Cell

The RNase PARN-1 Trims piRNA 3′ Ends to Promote Transcriptome Surveillance in *C. elegans*

Graphical Abstract

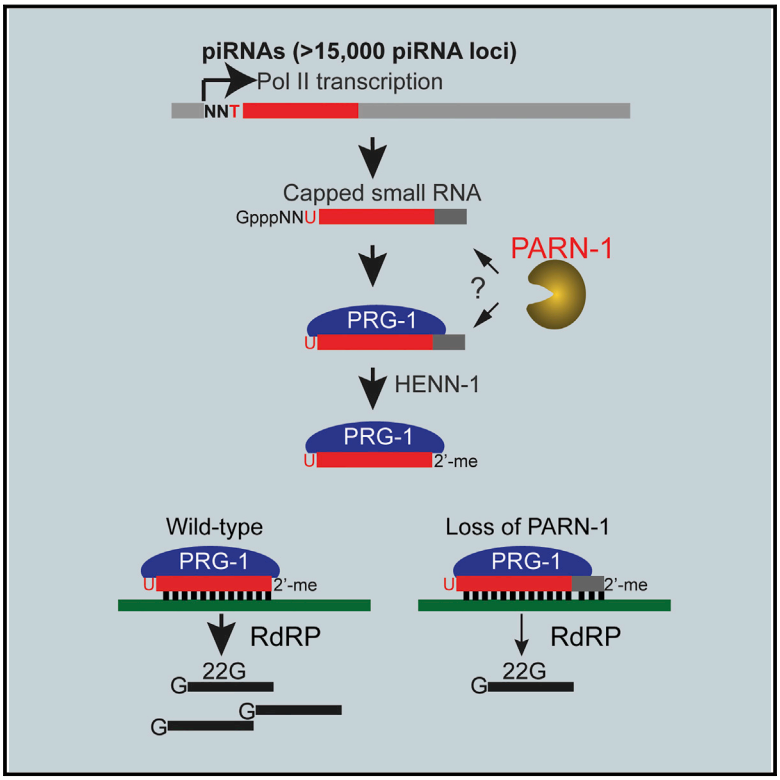

Highlights

- PARN-1 is required for piRNA 3′ end trimming in *C. elegans*
- PARN-1 is expressed in germline nuage and acts as a 3′ to 5′ exo-RNase
- 3′ trimming of piRNAs is important for both fertility and gene silencing

Authors

Wen Tang, Shikui Tu, Heng-Chi Lee, Zhiping Weng, Craig C. Mello

Correspondence

craig.mello@umassmed.edu

In Brief

In *C. elegans*, piRNA length is determined by the RNase PARN-1 and is important for piRNA-directed gene silencing.

Tang et al., 2016, Cell *164*, 974–984
February 25, 2016
http://dx.doi.org/10.1016/j.cell.2016.02.008

CellPress

Cell

Article

The RNase PARN-1 Trims piRNA 3′ Ends to Promote Transcriptome Surveillance in *C. elegans*

Wen Tang,[1] Shikui Tu,[2] Heng-Chi Lee,[1,4] Zhiping Weng,[2] and Craig C. Mello[1,3,*]
[1]RNA Therapeutics Institute
[2]Program in Bioinformatics and Integrative Biology
University of Massachusetts Medical School, Worcester, MA 01605, USA
[3]Howard Hughes Medical Institute
[4]Present address: Department of Molecular Genetics and Cell Biology, University of Chicago, Chicago, Illinois 60637, USA
*Correspondence: craig.mello@umassmed.edu
http://dx.doi.org/10.1016/j.cell.2016.02.008

SUMMARY

Piwi-interacting RNAs (piRNAs) engage Piwi proteins to suppress transposons and are essential for fertility in diverse organisms. An interesting feature of piRNAs is that, while piRNA lengths are stereotypical within a species, they can differ widely between species. For example, piRNAs are mainly 29 and 30 nucleotides in humans, 24 to 30 nucleotides in *D. melanogaster*, and uniformly 21 nucleotides in *C. elegans*. However, how piRNA length is determined and whether length impacts function remains unknown. Here, we show that *C. elegans* deficient for PARN-1, a conserved RNase, accumulate untrimmed piRNAs with 3′ extensions. Surprisingly, these longer piRNAs are stable and associate with the Piwi protein PRG-1 but fail to robustly recruit downstream silencing factors. Our findings identify PARN-1 as a key regulator of piRNA length in *C. elegans* and suggest that length is regulated to promote efficient transcriptome surveillance.

INTRODUCTION

Piwi proteins and Piwi-interacting RNAs (piRNAs) are essential for germline development and fertility in animals (Carmell et al., 2007; Cox et al., 1998; Houwing et al., 2007; Lin and Spradling, 1997). Although the genomic origins, lengths, and sequences of piRNAs are diverse between organisms, biogenesis mechanisms are remarkably conserved (Luteijn and Ketting, 2013; Weick and Miska, 2014). In worms, flies, and mice, for example, piRNA production involves primary piRNA pathways and amplification pathways that ensure robust silencing of their targets (Ishizu et al., 2012; Malone and Hannon, 2009; Senti and Brennecke, 2010; Siomi et al., 2011). Primary piRNA production requires 5′ and 3′ processing of piRNA precursors in each organism.

In flies and mice, primary piRNAs derive from piRNA clusters transcribed as single-stranded transcripts (Brennecke et al., 2007; Li et al., 2013; Malone et al., 2009). The endonucleases Zucchini (flies) and MitoPLD (mice) are thought to generate the 5′ ends of piRNAs (Ipsaro et al., 2012; Nishimasu et al., 2012; Olivieri et al., 2010; Pane et al., 2007). Precursor piRNA transcripts are bound by Piwi, which is thought to direct Zucchini/MitoPLD to cleave the primary transcript at a position 3′ downstream of the PIWI-bound region. In flies, Zucchini often generates ~26-nt intermediates that are compatible with Piwi binding (Han et al., 2015; Mohn et al., 2015). By contrast, piRNA intermediates generated by MitoPLD cleavage are 3–10 nt longer than mature piRNAs (Han et al., 2015; Mohn et al., 2015). The 3′ ends of intermediates, thus, are trimmed to the optimal length accommodated by Piwi (Kawaoka et al., 2011; Saxe et al., 2013; Vourekas et al., 2012). This trimming process requires an unknown exonuclease and the conserved Tudor-domain protein Papi/Tdrkh (Honda et al., 2013; Liu et al., 2011a; Saxe et al., 2013). The final step of piRNAs' maturation is the 2′-*O*-methylation at their 3′ termini that is catalyzed by the conserved methyltransferase Hen1 (Horwich et al., 2007; Kirino and Mourelatos, 2007; Saito et al., 2007).

The *C. elegans* Piwi protein PRG-1 binds piRNAs (termed 21U-RNAs) that derive from thousands of genomic locations, including two large clusters of piRNA genes on chromosome IV (Batista et al., 2008; Das et al., 2008; Gu et al., 2012; Ruby et al., 2006). The 21U-RNAs have a uniform length of 21 nt, a 5′ monophosphorylated (5′-monoP) uridine, and a 2′–*O*–methylated 3′ residue (Batista et al., 2008; Billi et al., 2012; Das et al., 2008; Kamminga et al., 2012; Montgomery et al., 2012; Ruby et al., 2006). The 21U-RNAs are processed from 25- to 29-nt capped small (cs) RNA precursors, which are transcribed by RNA polymerase II and initiate precisely 2 nt upstream of the 5′ end of mature 21U-RNAs (Cecere et al., 2012; Gu et al., 2012; Weick et al., 2014). Thus, to generate mature 21-nt piRNAs, the 5′ cap and first two nucleotides of a csRNA must be removed and extra nucleotides must be trimmed from the 3′ end. The enzymes that mediate the 5′ and 3′ processing of *C. elegans* piRNAs are unknown.

PRG-1 and its genomically encoded piRNAs scan for foreign sequences, while allowing mismatched pairing with the targets (Ashe et al., 2012; Bagijn et al., 2012; Lee et al., 2012a;

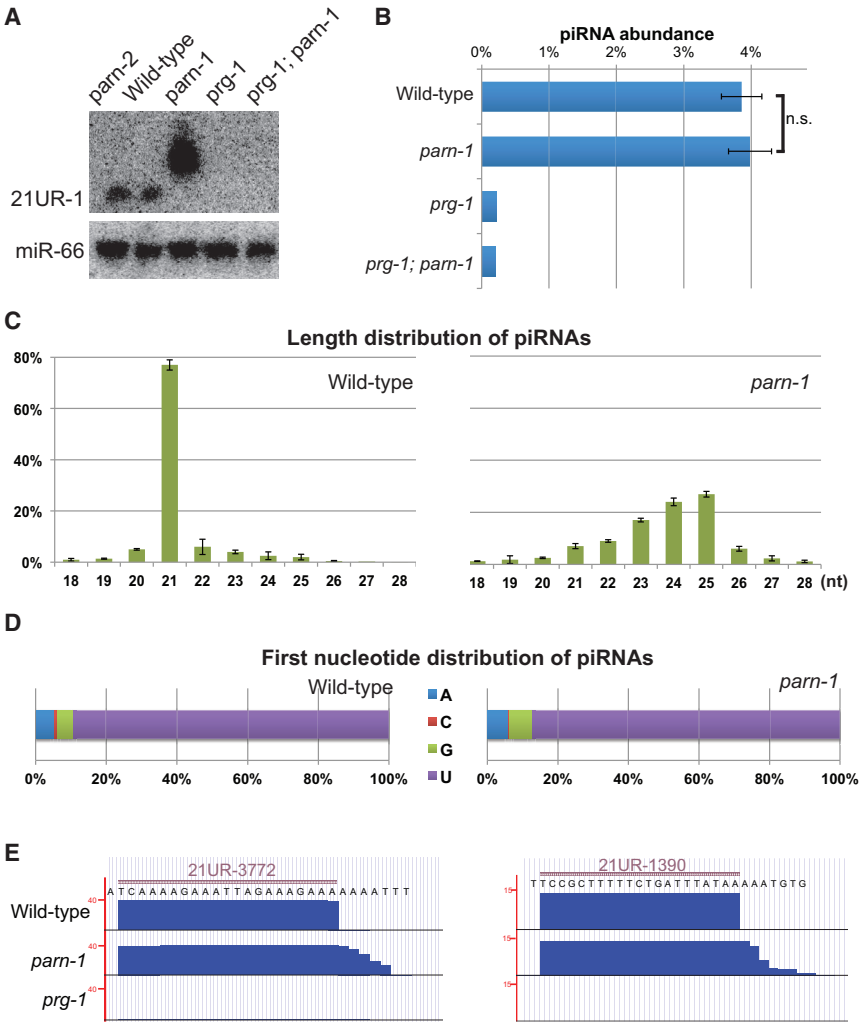

Figure 1. PARN-1 Is Required for 3′ Trimming of piRNAs

(A) Northern blot analysis of 21U-RNA-1 and miR-66 from total RNA prepared from WT, *parn-1*, *parn-2*, *prg-1*, and *parn-1; prg-1* double mutant strains.

(B) The expression profile for the bulk population of piRNAs as determined by small-RNA sequencing. Plotted for each library is the percent of reads that represented piRNAs after normalized to non-structural RNAs. For WT and *parn-1* samples, the average of three replicates is shown, error bars represent SEM. One set of small-RNA libraries from *prg-1* and *prg-1; parn-1* mutants is shown. n.s., not significant (Student's t test).

(C and D) Length distribution (C) and first nucleotide distribution (D) of piRNA reads from WT and *parn-1* mutant small-RNA libraries. The average of three experiments is shown, and error bars represent SEM.

(E) A browser view of representative piRNA loci. Small-RNA reads mapped the 21U-RNA-3772 and 21U-RNA-1390 genomic loci.

See also Figure S1

tures called P granules. Intriguingly, in *parn-1* mutants, untrimmed piRNAs associate with PRG-1 and accumulate to levels similar to those observed for wild-type (WT) piRNAs. Although the expression levels of piRNAs remain unchanged in *parn-1* animals, Piwi-dependent mRNA silencing is reduced, as is the production of Piwi-dependent 22G-RNAs on mRNA targets. Together, our findings demonstrate that the highly conserved PARN-1 protein is required for piRNA trimming and suggest that piRNA length is precisely regulated to promote Piwi/piRNA surveillance functions in the *C. elegans* germline.

Shirayama et al., 2012). For example, PRG-1 initiates epigenetic silencing on transgenes expressing the jellyfish green fluorescent protein (*gfp),* despite the fact that there are no perfectly matched piRNA target sites within the *gfp* sequence (Shirayama et al., 2012). "Self" mRNAs are protected from PRG-1 by the CSR-1 Argonaute pathway (Conine et al., 2013; Seth et al., 2013; Wedeles et al., 2013). Upon targeting, PRG-1 recruits RNA-dependent RNA polymerase (RdRP) to initiate the biogenesis of secondary small interfering RNAs (siRNAs), referred to as "22G-RNAs". The 22G-RNAs are then loaded onto worm-specific Argonautes (WAGOs) to maintain and propagate epigenetic silencing (Ashe et al., 2012; Bagijn et al., 2012; Lee et al., 2012a; Shirayama et al., 2012).

Here, we show that PARN-1, a conserved exonuclease, is required for 3′-end processing of piRNA in *C. elegans*. Recombinant PARN-1 protein possesses 3′-to-5′ exonuclease activity in vitro. Depletion of PARN-1 specifically compromises 3′ trimming of piRNAs while 5′ end processing and methylation of 3′ ends are unaffected. PARN-1 is restricted to the adult germline and co-localizes with PRG-1 in germline nuage struc-

RESULTS

PARN-1 is Required for piRNA Trimming

To identify RNases responsible for 3′ end trimming, we took a candidate approach. We used northern blotting to search for changes in piRNA length in animals depleted for expression of candidate nucleases. This search identified PARN-1 as specifically required for piRNA expression in *C. elegans* (Figures 1A and S1A). Animals bearing a presumptive null allele of *parn-1*(*tm869*), which deletes most of the catalytic domain and shifts the open reading frame (Nousch et al., 2013), failed to express mature 21U-RNAs and instead produced piRNA species several nucleotides longer (Figures 1A and S1B). Mutations in another *parn* gene, *parn-2,* had no effect on piRNAs and failed to enhance the piRNA defect *of parn-1* mutants (Figures 1A and S1B). Expression of a *parn-1::gfp* transgene restored expression of piRNAs of appropriate length (Figure S1B).

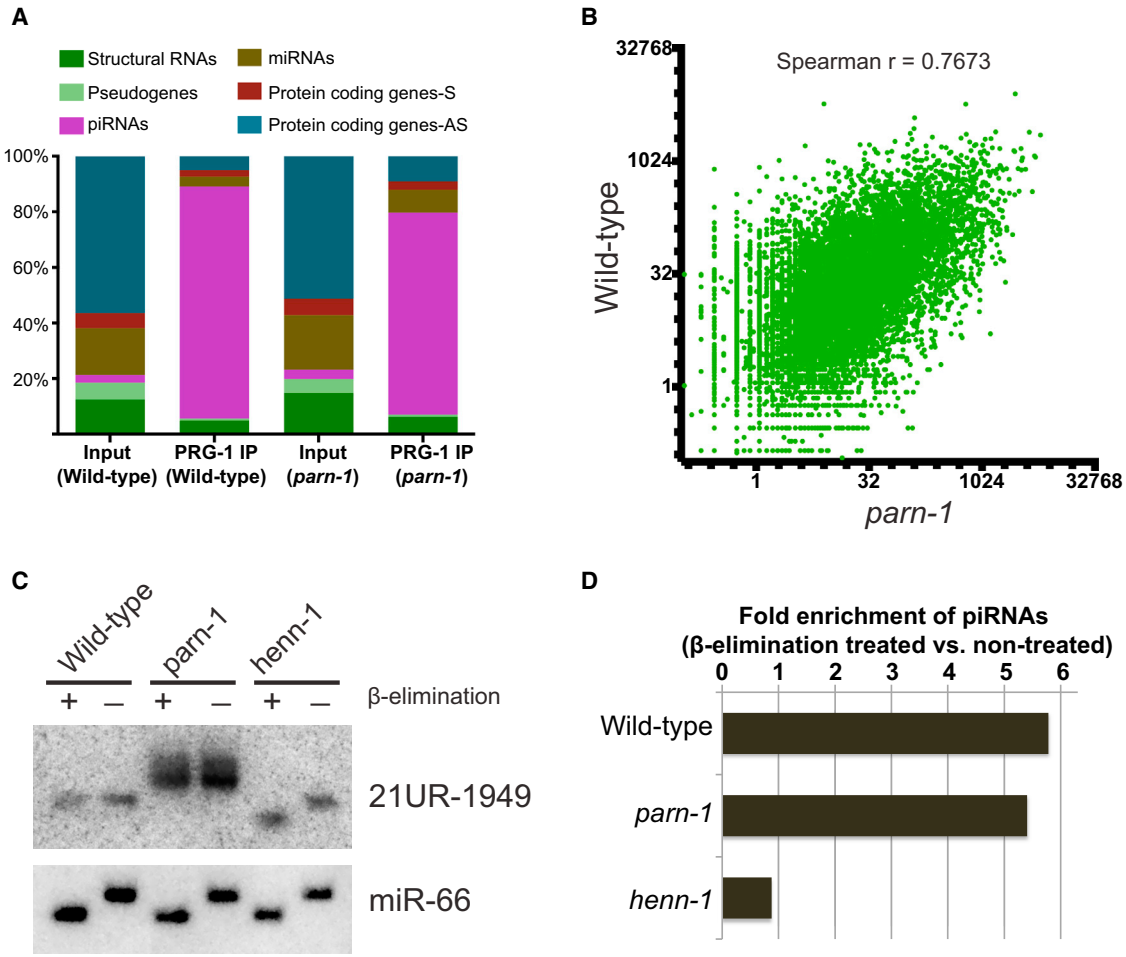

Figure 2. Untrimmed piRNAs Are Loaded onto PRG-1 and Possess 2′-O-Methylation

(A) Bar plots showing the change in small-RNA reads matching indicated genome annotations between input and PRG-1 IP samples prepared from WT and *parn-1* strains.

(B) Correlation analysis of the piRNA level. Libraries were prepared from PRG-1 IP samples from WT and *parn-1* strains. Data from reads for each piRNA were normalized to total reads in the same sample. For a perfect correlation, the Spearman rank correlation coefficient (r) = 1 or −1 and, for no correlation, r = 0.

(C) Oxidation and β-elimination followed by northern blot analysis of RNA prepared from WT, *parn-1*, and *henn-1* strains. RNA samples were not treated (−) or β-elimination treated (+) and probed for 21UR-1949. Probing for miRNA-66 served as controls for loading and β-elimination reactions.

(D) Fold enrichment of piRNA reads was calculated by comparing β-eliminated and non-treated samples. Small RNA libraries were generated from β-eliminated and untreated RNAs prepared from WT, *parn-1*, and *henn-1* strains.

See also Figure S2

Previous studies showed that piRNA accumulation depends on PRG-1, suggesting that PRG-1 protects and stabilizes piRNAs in WT animals (Batista et al., 2008; Das et al., 2008; Wang and Reinke, 2008). Consistent with the idea that the longer *parn-1* mutant piRNAs are also stabilized by PRG-1, our northern blots revealed that *prg-1; parn-1* double mutants lack piRNAs (Figure 1A). To look more broadly at small-RNA biogenesis in *parn-1* mutants, we cloned and deep sequenced small RNAs. We employed three different small-RNA cloning methods. To enrich for 5′-monoP species such as microRNAs (miRNAs) and piRNAs, we employed a direct ligation method to add a 5′ adaptor. To recover small RNAs with capped or 5′ triphosphorylated (5′ triP) ends, we applied two additional protocols, one involving pre-treatment with 5′ Polyphosphatase, which removes the γ and β phosphates from 5′-triP RNA, and a second involving pre-treatment with tobacco acid pyrophosphatase (TAP) to convert 5′ capped or polyphosphate RNA into 5′-monoP RNA. Using all of these methods, we found that overall piRNA abundance was comparable between WT and *parn-1* strains (Figures 1B and S1C). Interestingly, the piRNAs in *parn-1* mutants were extended by 2–4 nts at their 3′ ends but exhibited 5′ ends that map precisely to the 5′ uridine of WT mature piRNAs (Figures 1C and 1D). This finding was further confirmed by inspecting specific piRNA loci (Figure 1E). No changes in the length distribution of other small RNA species, such as miRNAs, were observed (Figures 1A and S1D). As expected, piRNA levels were dramatically reduced in *prg-1* single mutant and *prg-1; parn-1* double mutant animals (Figures 1A, 1B, and S1B).

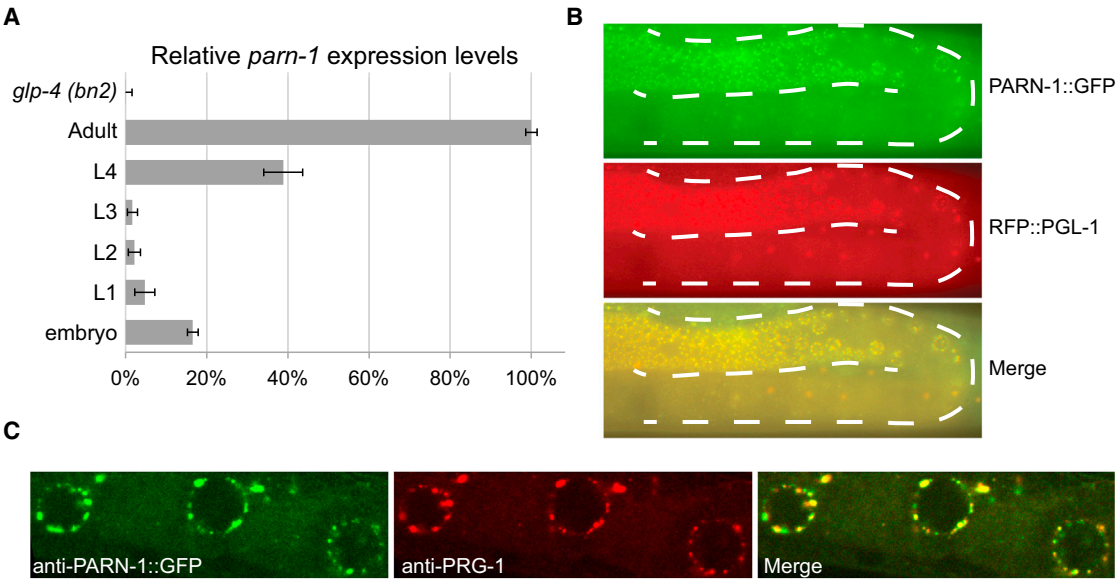

Figure 3. PARN-1 Is Expressed in the Germline and Localizes in P Granules

(A) qRT-PCR of *parn-1* mRNA from total RNA isolated from synchronized WT populations at the indicated developmental stages and germline-deficient *glp-4 (bn2)* mutants at the adult stage. Expression of *act-3* served as the internal control. Data were collected from three independent biological replicates. Error bars represent SD.

(B) Fluorescence micrographs showing PARN-1::GFP expression (green) from an adult hermaphrodite. Expression of RFP::PGL-1 (red) served as the P granule marker. The dashed lines outline the position of the germline.

(C) Immunostaining of PRG-1 (red) and PARN-1::GFP (green) in dissected gonad arms from the *parn-1::gfp* rescue line.

See also Figure S3

Although our northern blots suggest that untrimmed piRNAs are more abundant than WT piRNAs (Figures 1A and 2C), our deep-sequencing data do not support this conclusion. It is possible that the stronger signals on northern blots do not reflect increased levels but rather stronger hybridization, perhaps due to pairing between the additional 3′ nucleotides in the longer piRNAs and the flanking sequences present in the Starfire probes (Integrated DNA Technologies). Altogether, our findings suggest that PARN-1 is required for 3′ trimming, but not for 5′ processing.

To ask whether the untrimmed piRNAs associate with PRG-1, we recovered PRG-1 immunoprecipitation (IP) complexes from *parn-1* extracts and analyzed PRG-1-bound small RNAs through deep sequencing. We found that the longer piRNAs co-precipitated with PRG-1 and confirmed their extended 3′ ends and their 5′ uridine (Figures 2A, S2A, and S2B). The majority of piRNA species exhibited significant enrichment in the PRG-1 IP complex, and the levels of the untrimmed piRNA species correlated well with that of their corresponding WT counterparts (Figures 2B, S2C, and S2D). Similarly, we found that the expression levels of PRG-1 protein appeared similar in WT and *parn-1* mutant animals as assayed by western blotting (Figure S2E).

To examine the methylation status of piRNA 3′ ends, we performed β-elimination experiments. While RNAs containing 2′ and 3′ hydroxyl groups react with sodium periodate, RNA species with terminal 2′-O-methylation are resistant to this treatment. The β-elimination reaction removes the last nucleotide leaving a phosphate group at the 3′ terminus. The resulting size change can be monitored by PAGE. Interestingly, we found that piRNAs were methylated in WT and *parn-1* animals, but not in the *henn-1* methyltransferase mutant (Figure 2C) (Billi et al., 2012; Kamminga et al., 2012; Montgomery et al., 2012). A control miRNA known to have terminal 2′ hydroxyl showed the expected size shift in both WT and in *parn-1* mutants (Figure 2C). To determine whether resistance to sodium periodate treatment is a general feature of these longer piRNAs, we deep sequenced both β-eliminated and untreated small RNAs harvested from WT, *parn-1*, and *henn-1* strains. This treatment leaves a 2′-phosphate at the 3′ end of RNAs containing 2′ and 3′ hydroxyl groups, rendering them poor substrates for 3′ adaptor ligation. Thus, non-modified RNA species are eliminated, while RNAs with terminal 2′-O-methylation are expected to be enriched in deep-sequencing libraries generated from periodate-treated samples. We found that periodate treatment enriched the abundance of piRNAs by 5- to 6-fold in both WT and *parn-1* animals when compared to untreated samples (Figure 2D). These enrichments were not observed in *henn-1* mutants (Figure 2D). Thus, although untrimmed at their 3′ ends, the piRNAs in *parn-1* animals are properly loaded onto PRG-1 and exhibit 5′ and 3′ end structures typical of WT piRNAs.

PARN-1 Localizes in Germline Nuage

We next examined *parn-1* mRNA expression and PARN-1 protein localization. Using qPCR, we found that *parn-1* mRNA was expressed at low levels at the L1 to L3 larval stages but began to accumulate at the L4 stage and reached its highest expression level at the gravid adult stage (Figure 3A). We found that *parn-1* mRNA was not detected in RNA samples isolated

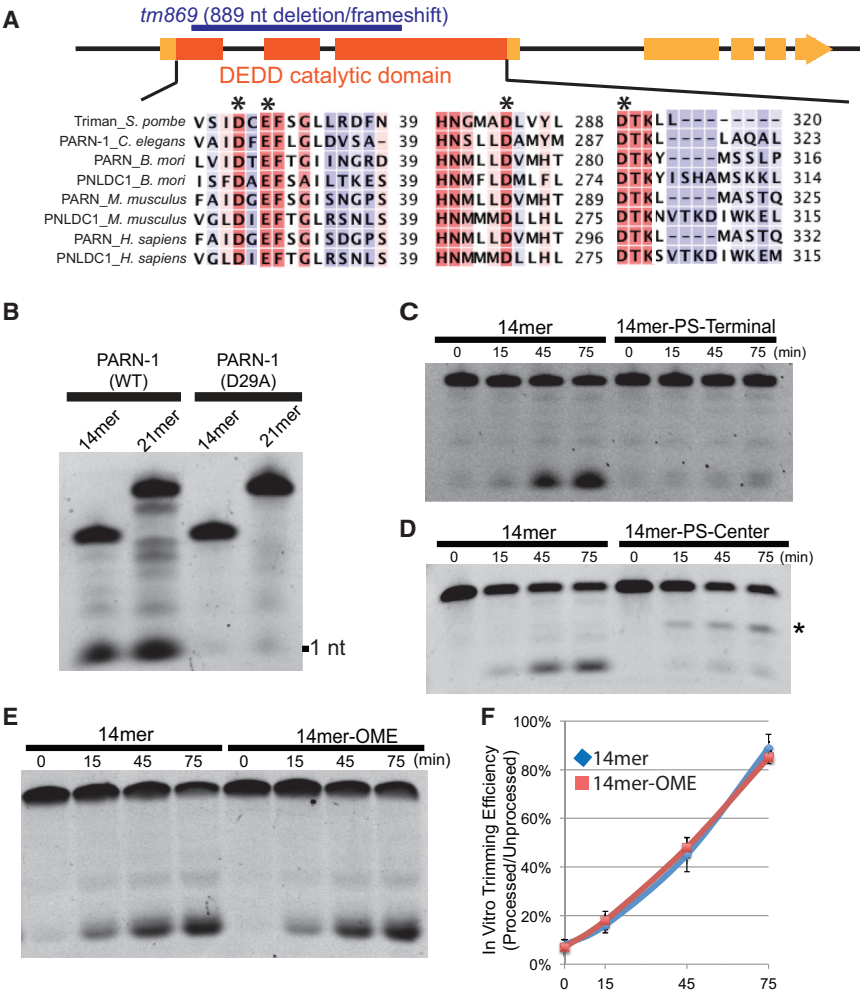

Figure 4. Recombinant PARN-1 Possesses 3′-to-5′ Exonuclease Activity In Vitro

(A) Schematic of the *parn-1* genes showing exons (boxes) and introns (lines) with the catalytic RNase domain shaded in dark orange. The deletion allele (*tm869*) is highlighted in blue. The alignment shows human, mouse, *C. elegans*, *B. mori*, and *S. pombe* PARN and PNLDC with conserved catalytic residues (asterisk).

(B) Electrophoresis analysis on 21-nt and 14-nt 5′ fluorescein-labeled RNA substrates incubated with purified PARN-1 (WT and D29A) proteins.

(C–E) Electrophoresis analysis of 14-mer RNAs containing 3′ hydroxyl (14-mer) and PS bonds from positions 10 to 14 (14-mer-PS-Terminal) (C), 14-mer RNAs with PS bond between positions 7 to 8 (14-mer-PS-Center). Asterisk represents the degradation intermediate (D) and 14 mers containing 3′ hydroxyl and 2′–O–methylated 3′ termini (14-mer-OME) (E).

(F) Quantification of the ratio between processed and unprocessed products among biological replicates. The average of six replicates for 14 mer and the average of three replicates for 14-mer-OME are shown. Error bars represent SD.

See also Figure S4

from germline-deficient *glp-4 (bn2)* animals (Beanan and Strome, 1992), suggesting that expression of *parn-1* is restricted to the germline (Figure 3A). PRG-1 protein was previously shown to localize in P-granules (Batista et al., 2008; Wang and Reinke, 2008), where surveillance of nascent transcripts as well as piRNA maturation may take place (Klattenhoff and Theurkauf, 2008; van der Heijden et al., 2010). We found that a rescuing PARN-1::GFP substantially co-localized with PRG-1 and with the P granule component, PGL-1 (Figures 3B and 3C) (Kawasaki et al., 1998). In some instances, we observed PARN-1 localization adjacent to PRG-1 rather than fully overlapping with PRG-1 foci (Figure 3C). PRG-1 localization appeared to be WT in *parn-1* mutants (Figure S3A), and similarly, PARN-1::GFP localization was not altered in PRG-1 mutants (Figure S3B). Thus, PRG-1 and PARN-1 can both independently localize to P-granules.

Although the proteins co-localize in germline nuage, we failed to detect physical interactions between PRG-1 and PARN-1::GFP in co-immunoprecipitation assays (Figure S3C). These findings suggest that the PARN-1-mediated piRNA trimming either occurs prior to PRG-1 loading or is very transient.

PARN-1 Is a 3′ to 5′ Exo-RNase

PARN-1 belongs to a highly conserved RNase family that contains the DEDD catalytic domain (Figure 4A) (Goldstrohm and Wickens, 2008; Körner et al., 1998; Zuo and Deutscher, 2001). To directly test whether PARN-1 functions as an RNase, we purified the PARN-1 protein in *Escherichia coli* (Figure S4A). We found that recombinant WT PARN-1 processed 5′-end-labeled synthetic RNA substrates of 14 and 21 nts into variable sized fragments with a prominent product of one nucleotide (Figure 4B). To rule out the possibility that the observed activity was catalyzed by a contaminating bacterial nuclease, we also expressed a *parn-1* mutant in which the conserved aspartic acid residue (D29) was mutated to alanine. As expected, this D29A catalytic mutant showed greatly reduced nuclease activity in our in vitro assay (Figure 4B). To test whether PARN-1 is an exo-RNase, we used 14-mer oligonucleotides with phosphorothioate (PS) linkages. PS bonds are known to stabilize oligonucleotides against nuclease degradation (Kawaoka et al., 2011; Ren et al., 2004). Incorporation of PS linkages at the 3′ end should therefore render the substrate resistant to 3′ exo-RNase trimming but should leave it sensitive to endo-RNases. We found that the 14-mer-PS-terminal substrate exhibited a significant reduction in processing compared to an unmodified control (Figure 4C). Consistent with the idea that PARN-1 acts as a 3′-5′ exo-RNase, when the PS bond was instead placed between positions 7 and 8 (14-mer-PS-Center), trimming of the substrate was blocked specifically at the PS site (Figure 4D).

By incubating PARN-1 with varying concentrations of substrate, we determined its Michaelis-Menten parameter K_M value to be 18 nM. To test whether the enzyme is a processive enzyme,

different amounts of the substrate (18 and 108 nM, corresponding to concentrations at or in 6-fold excess of the Km value) were subjected to the trimming assay. Two findings indicate PARN-1 trims RNA in a processive mode: (1) in the time course experiment, both RNA substrate and fully processed product are present at some time points, and (2) more importantly, the time point for the appearance of the first fully processed product is independent of the amount of RNA substrate in the reaction (Figure S4B).

We next wished to ask whether recombinant PARN-1 could process untrimmed piRNAs associated with PRG-1. We purified PRG-1 complexes by PRG-1 IP and by FLAG IP from *parn-1* mutant extracts and incubated these purified complexes with recombinant PARN-1. To monitor for potential inhibitory factors present in the reaction that might inactivate the recombinant RNase, we included a labeled "naked" RNA substrate as a positive control. While the naked substrate was efficiently processed, we failed to detect any significant trimming of the piRNAs associated with PRG-1 immune complexes (Figure S4C). To ask whether the methylated 3′ termini of these PRG-1 bound piRNAs block 3′ trimming, we conducted trimming experiments using PRG-1 complexes purified from *henn-1; parn-1* double mutants. We found that unmethylated piRNAs in these PRG-1 complexes were also resistant to trimming by recombinant PARN-1 (Figure S4C). Moreover, we found that when incubated with a naked RNA containing a 3′ terminal methylation, purified PARN-1 digested the substrate at a rate similar to that observed for an unmodified substrate (Figures 4E and 4F). These findings suggest that 2′-O-methylation does not protect piRNAs from PARN-1 processing. Instead, the 3′ ends of the untrimmed piRNAs appear to be protected by PRG-1 binding, perhaps by association with the PAZ domain of PRG-1 (Simon et al., 2011; Tian et al., 2011).

PARN-1 Is Required for Fertility and Acts in the PRG-1 Pathway

Mutations in Piwi pathway components cause reduced fertility in *C. elegans* (Batista et al., 2008; Das et al., 2008; Wang and Reinke, 2008). In *prg-1* animals, this sterility phenotype is progressive and fertility declines over generations (Barberán-Soler et al., 2014; Simon et al., 2014). To accurately measure fertility in different mutant backgrounds, we outcrossed the *prg-1* and *parn-1* strains with WT four times and freshly generated the *prg-1; parn-1* double mutants prior to scoring brood sizes. Consistent with findings from a previous study (Nousch et al., 2013), we found that *parn-1* animals display a reduced brood size at elevated temperature (25°C) as compared to WT (Figure 5A). Fertility was rescued to WT levels by expression of a *parn-1::gfp* transgene (Figure 5A). The reduced fertility observed in *parn-1* mutants was less than that observed in *prg-1* mutants (Figure 5A).

PARN-1 homologs regulate gene expression independently of piRNAs in other species (Berndt et al., 2012; Copeland and Wormington, 2001; Lee et al., 2012b), thus it was possible that the fertility defect of *parn-1* is not caused by the observed defect in trimming piRNAs. We therefore used a genetic epistasis test to ask whether PARN-1 acts in the *prg-1* pathway. If the fertility defects observed in *parn-1* animals results from defects in functions unrelated to piRNA processing, the phenotype of the double mutant would be expected to exhibit an additive fertility deficit. However, in contrast to this possibility and consistent with their function within the same pathway, we found that *parn-1; prg-1* double mutants exhibited fertility levels similar to those observed in *prg-1* single mutants (Figure 5A). These findings suggest that PARN-1 acts in the Piwi pathway and is required for fertility and, furthermore, that the PRG-1-bound untrimmed piRNAs must retain at least partial function.

parn-1 Mutants Are Partially Defective in Transgene Silencing and 22G-RNA Production

To ask whether *parn-1* mutants are defective in transgene silencing, we first tested a *gfp::cdk-1* transgene that is exceptionally prone to silencing in WT animals (Shirayama et al., 2012). As expected, we found that introduction of this transgene into WT animals invariably resulted in silencing (n = 5), while introduction into *prg-1* mutant animals resulted in uniform and robust expression of the nuclear GFP::CDK-1 protein (n = 4; Figure 5B) (Shirayama et al., 2012). Strikingly, and consistent with a role for *parn-1* in the PRG-1 pathway, we found that newly introduced copies of the *gfp::cdk-1* transgene were stably expressed in all of the independently generated *parn-1* mutant transgenic strains analyzed (n = 6; Figure 5B).

We next asked whether *parn-1* mutants were defective in piRNA guided silencing of a perfectly matched target. For this assay, we used a *gfp::h2b* reporter engineered to contain sites perfectly complementary to two abundant piRNAs (Figure 5C). As previously reported (Lee et al., 2012a), this transgene was silenced when introduced into WT animals but was active upon introduction into *prg-1* mutants (Figure 5C). Interestingly, however, *parn-1* mutants were able to silence this *gfp::h2b* transgene (Figure 5C). The polynucleotide polymerase RDE-3 is required for the accumulation of WAGO 22G-RNAs (Chen et al., 2005; Gu et al., 2009), and as expected, we found that crossing the silent reporter from WT or *parn-1* mutants into the *rde-3* animals resulted in fully restored transgene expression (Figure 5C). Taken together, these data suggest that untrimmed piRNAs have reduced activity but can, nevertheless, recognize perfectly complementary sequences to initiate 22G-RNA biogenesis and target silencing.

In addition to stimulating 22G-RNA production on transgenes with foreign sequences, PRG-1 also triggers 22G-RNA production on endogenous RNA targets (Bagijn et al., 2012; Lee et al., 2012a). We therefore examined whether depletion of PARN-1 affects synthesis of these PRG-1-dependent 22G-RNAs on endogenous genes. There are 1,478 genes that exhibit a depletion of 22G-RNAs in *prg-1* mutants when compared to WT (Figure 6A; Table S2). Strikingly, a significant overlap was found between genes with depleted 22G-RNAs in *parn-1* animals and genes previously identified as *prg-1* targets (Figure 6A; Table S2). Consistent with *parn-1* and *prg-1* functioning together on these targets, *parn-1; prg-1* double mutants also exhibited a very significant overlap with *prg-1* single mutants (Figure 6A; Table S2). Finally we found that 22G-RNAs at predicted target sites were significantly reduced in *parn-1* mutant animals (Figure 6B; Table S3). Depletion of 22G-RNAs was not observed at

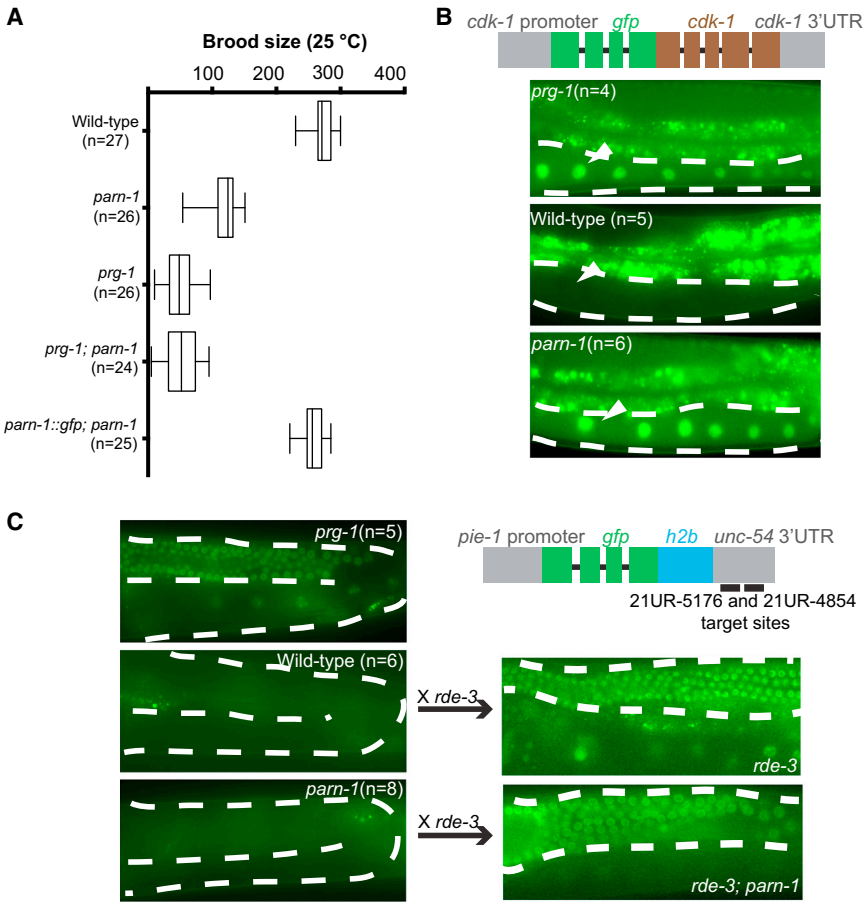

Figure 5. PARN-1 Is Required for Fertility and Epigenetic Silencing of Single-Copy Transgenes

(A) Brood size counts in WT, *prg-1*, *parn-1*, *prg-1; parn-1* double, and *parn-1* rescue animals at 25°C. n, number of parental adults scored.

(B and C) Schematics of the *gfp::cdk-1* reporter (B) and of the *h2b::gfp::21U-RNA-target-site* reporter (C) that were injected into wild-type, *parn-1*, and *prg-1* worms to establish single-copy transgenic lines. Images of GFP fluorescence signals in the resulting strains are shown. Oocyte nuclei that either express or fail to express the construct are indicated by arrowheads. The dashed lines outline the position of germline. Bright signals outside of the germline are from gut granule autofluorescence. The *gfp::h2b::21U-RNA-target-site* reporter established in WT and *parn-1* animals was crossed to the *rde-3* mutant strain. n, number of independent transgenic lines exhibiting the pattern of expression shown.

randomly selected sites (Figures S5A and S5B). Consistent with the idea that the longer piRNAs produced in *parn-1* mutants are partially functional, we found that, although reduced relative to WT, 22G-RNAs were nevertheless enriched relative to *prg-1* mutants near predicted piRNA target sites (Figure 6C). Taken together these findings suggest that untrimmed piRNAs, despite their robust loading onto PRG-1, exhibit reduced activity in both 22G-RNA induction and target silencing.

DISCUSSION

A Conserved Role for PARN Family Members in piRNA Processing

PARN was initially identified as a poly(A)-specific 3′ exo-RNase (Aström et al., 1992; Körner and Wahle, 1997; Körner et al., 1998). In *C. elegans* the Ccr4-Not deadenylase complex, rather than PARN-1, appears to be the key regulator of poly(A) tail length (Nousch et al., 2013). Here, we have shown that the *C. elegans* PARN ortholog, PARN-1, is the bona fide 3′ trimmer for piRNAs in *C. elegans*. Both the Human and mouse genomes contain PARN, and a second homolog named poly(A)-specific RNase-like domain containing 1 (PNLDC1) (Figure 4A). While mouse PARN appears to be ubiquitously expressed in all tissues, PNLDC1 is enriched in mouse testes (Brawand et al., 2011; Petryszak et al., 2014), making it a good candidate for a role in piRNA processing. Finally, an independent study has identified the PARN family member PNLDC1 from silkworm *Bombyx mori* as an RNase required for piRNA trimming (Izumi et al., 2016 [in this issue of *Cell*]). Together, these findings suggest that, despite the many differences in piRNA gene organization and the different lengths of mature piRNAs in mammals, insects, and nematodes, the machinery for defining piRNA length may nevertheless be conserved.

The PARN family of RNases belongs to the DEDD exonuclease superfamily whose members have diverse functions in processing both RNA and DNA (Goldstrohm and Wickens, 2008; Zuo and Deutscher, 2001). Several members of the DEDD family play important roles in small-RNA silencing. For example, in worms, MUT-7 is required for RNAi, although its biochemical function is unknown (Gu et al., 2009; Ketting et al., 1999; Tabara et al., 1999). In flies, Nibbler modulates the lengths of some miRNAs and piRNAs (Feltzin et al., 2015; Han et al., 2011; Liu et al., 2011b). In fission yeast, Triman, a PARN family member, processes Dicer-independent small RNAs that are involved in heterochromatin establishment (Marasovic et al., 2013). In vertebrates, PARN mediates 3′-end formation of an Ago2-cleaved miRNA (Yoda et al., 2013). Given the diversity of both proteins themselves and distinct functions of their small-RNA substrates, these examples could represent convergent evolution rather than conservation of a role in small-RNA processing.

What Determines piRNA Size?

Our findings support a model for piRNA biogenesis in *C. elegans* in which the exonuclease PARN-1 mediates 3′ trimming of piRNA precursors prior to, or independently from, PRG-1 loading (Figure 6D). In vitro reconstitution in silkworm cell extracts suggested that 3′ trimming occurs on Piwi-bound piRNA precursors (Kawaoka et al., 2011). Consistent with this notion, depletion of

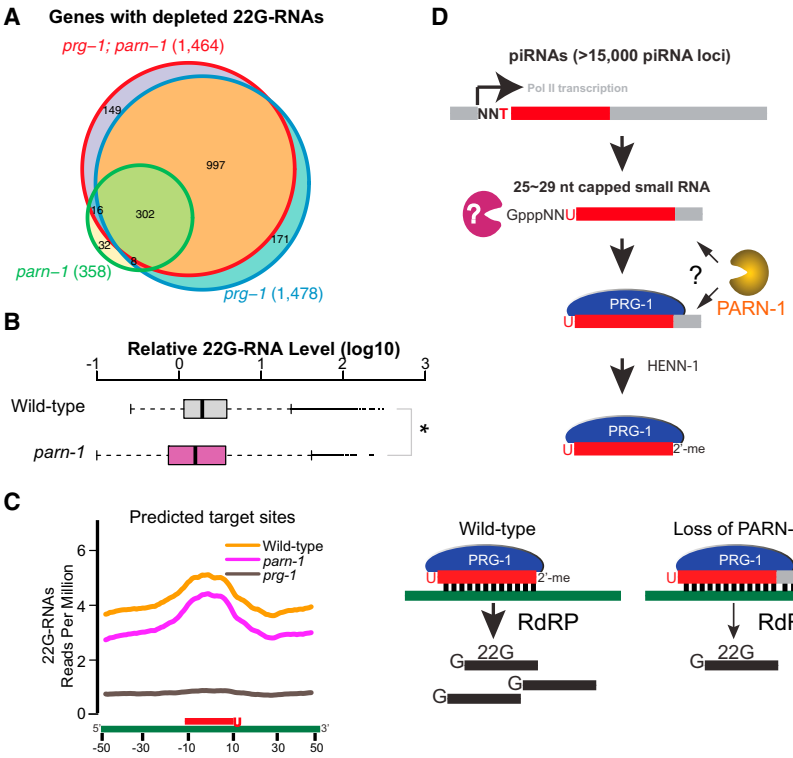

Figure 6. Trimming of piRNAs Is Important for 22G-RNAs Production

(A) Venn diagram summarizing the overlap in the number of genes whose 22G-RNA levels decrease by 2-fold when compared to WT. Gene sets from *prg-1*, *parn-1*, and *prg-1; parn-1* double mutants are plotted (p values < 0.0001; hypergenomic test).

(B) Box-and-whisker plot showing fold change of 22G-RNAs at predicted target sites in WT and *parn-1* mutants as compared to *prg-1* mutants. Asterisks indicate statistical significance (p value = $6.26 \times e^{-227}$, Wilcoxon Rank-Sum Test).

(C) Density of 22G-RNAs in a 100-nt interval around predicted piRNA target sites in the WT, *parn-1*, and *prg-1* mutants. The plots are centered on piRNAs.

(D) Model illustrating the role of PARN-1 in piRNA biogenesis and functions.

See also Figure S5 and Tables S2 and S3

Tdrkh/Papi, a Tudor domain protein that presumably recruits the trimmer, leads to longer piRNAs that are associated with Piwi proteins (Han et al., 2015; Mohn et al., 2015; Saxe et al., 2013). Our findings demonstrate that, once loaded on PRG-1, untrimmed piRNAs are as stable as WT piRNAs, are at least partially functional, and have the terminal 2′–O–methyl modification normally found on mature piRNAs. Thus, in WT animals, PARN-1-mediated trimming prevents longer piRNAs from being loaded and stabilized on PRG-1. The finding that recombinant PARN-1 processes naked RNA down to single nucleotides suggests that PRG-1 or other factors may be required to limit PARN-1 processing in vivo.

Properties of Untrimmed piRNAs

Compared to their WT counterparts, piRNAs in *parn-1* mutants are only slightly (2–4 nts) longer. Yet, these longer piRNAs are defective in several Piwi pathway activities. First, *parn-1* animals have reduced fertility at elevated temperature. Second, the silencing of foreign sequences, such as the *gfp::cdk-1* transgene, is compromised. Lastly, the accumulation of PRG-1-dependent 22G-RNAs is significantly reduced. For miRNAs, base-pairing within the 3′ region can supplement pairing within the seed region (nucleotides 2–8) (Bartel, 2009; Brennecke et al., 2005; Friedman et al., 2009). In vitro studies suggest that release of the target RNA is a slow step in Argonaute-guided catalysis (Deerberg et al., 2013; Haley and Zamore, 2004; Salomon et al., 2015). Extended base-pairing between targets and the longer piRNAs in *parn-1* may over-stabilize target interactions, reducing the ability of PRG-1 to efficiently scan germline transcripts. Considering the uniformity of piRNA length in WT animals, our findings reveal a surprising versatility in the ability of PRG-1 to accommodate and protect piRNAs of different length. Thus, the stereotypical size of piRNAs in *C. elegans,* and perhaps in other animals, may reflect precise regulation of the trimming machinery rather than a limitation imposed by physical attributes of the Piwi proteins themselves. Our findings suggest that the optimal sizing of piRNAs is important for both fertility and gene silencing.

EXPERIMENTAL PROCEDURES

Strains and Genetics

C. elegans culture and genetics were performed as described (Brenner, 1974). The Bristol strain N2 was used as the standard WT strain. Alleles used in this study listed by chromosome: LGI: *prg-1(tm872)*, *glp-4(bn2)*; LGII: *parn-2(tm1339)*, neSi[*cb-unc-119(+); wago1p::parn-1::gfp*], neSi[*cb-unc-119(+); flag::prg-1*]; LGIII: *henn-1(tm4477)*; LGV: *parn-1(tm869)*; and unmapped: *rfp::pgl-1*. Depletion of candidate nucleases was conducted by feeding worms bacteria expressing double-stranded RNA (dsRNA) as described (Conte et al., 2015).

Generation of Transgenic Lines by MosSCI

The *gfp::cdk-1* (Shirayama et al., 2012) and *gfp::h2b* (Lee et al., 2012a) reporters were injected into recipient strains EG4322 *Mos1(ttTi5605)* II; *unc-119(ed3)* III, TW35 *Mos1(ttTi5605)* II; *unc-119(ed3)* III; *parn-1(tm869)* V and TW60 *Mos1(ttTi5605)* II; *unc-119(ed3)* III; *prg-1 (tm872)* I using a direct insertion method (Frøkjaer-Jensen et al., 2008).

To generate the MosSCI donor vector for *parn-1::gfp* integration, *wago-1* promoter sequences (1159 bp), *wago-1* 3′ UTR (360 bp) *parn-1* open reading frame sequences, and *gfp* coding sequences were sequentially cloned to pBluescript SK (+). PARN-1 mutants (D29A and D29A; E31A) were generated by Q5 site-directed mutagenesis kit (New England Biolabs). The fragment was subcloned into the MosSCI vector pCFJ151. The transgenic lines were generated as described (Frøkjaer-Jensen et al., 2008).

Small RNA Cloning

Total RNA was extracted from adult N2 and outcrossed mutants at generation twelve using TRI Reagent (Molecular Research Center). Small RNA was enriched using MirVana Kit (Life Technologies). RNAs ranging from 18–40 nt were further purified from the 15% polyacrylamide/7M urea gel. RNAs from

WT, *parn-1*, *prg-1*, *parn-1; prg-1* double mutants, and input and IP samples were subjected to TAP (Epicenter) treatment, RNA 5′ polyphosphatase (Epicenter) treatment, or mock treatment. All small RNAs were ligated to the miRNA cloning linker 1 (5′ rAppCTGTAGGCACCATCAAT/3ddC/ 3′, IDT) and a 5′ linker containing a 4-nt barcode using T4 RNA ligase (Takara). Ligated RNA products were converted to cDNA using Superscript III Reverse Transcriptase (Life Technologies). Libraries were amplified and sequenced using HiSeq sequencing system (Illumina) at the University of Massachusetts Medical School Deep Sequencing Core.

β-Elimination Reaction

The MirVana Kit (Life Technologies) enriched 50 μg of small RNA. The enriched 50 μg of small RNA was incubated with borax/boric acid buffer (0.06 M borax, 0.06 M boric acid, [pH 8.6]) containing 25 mM $NaIO_4$ at room temperature for 1 hr. We added 20 μl of 50% glycerol to quench extra $NaIO_4$. RNA was collected by ethanol precipitation. The pellet was dissolved in 100 μl borax/boric/NaOH buffer (0.055 M borax, 0.055 M boric acid, 0.055 M NaOH, [pH 9.5]) and incubated at 45 °C for 90 min. RNA was recovered by ethanol precipitation and subjected to small-RNA cloning and northern analysis.

Protein Purification

The cDNA-encoding truncated PARN-1 containing the catalytic domain (residue 1–403) were cloned into the pGEX-4T-3 vector (GE Healthcare) and the mutated PARN-1 (D29A) was generated by Q5 site-directed mutagenesis kit (New England Biolabs). Proteins were expressed as the glutathione-S transferase fusion protein in ArcticExpress cells (Agilent Technologies) at 12°C overnight and purified using glutathione sepharose 4B (GE Healthcare). Recombinant proteins were dialyzed against RNA trimming buffer (20 mM HEPES-KOH [pH 7.5], 50 mM KCl, 0.25 mM $MgCl_2$, 1 mM DTT), supplemented with 20% glycerol, and stored at −80°C. Protein purity was examined by SDS-PAGE followed by Coomassie blue staining.

ACCESSION NUMBERS

The accession numbers for the sequencing data reported in this paper is Archive (SRA): SRS1021265.

SUPPLEMENTAL INFORMATION

Supplemental Information includes Supplemental Experimental Procedures, five figures, and three tables and can be found with this article online at http://dx.doi.org/10.1016/j.cell.2016.02.008.

AUTHOR CONTRIBUTIONS

Conceptualization, W.T., Z.W., and C.M.; Investigation, W.T., S.T., and H.-C.L.; Writing – Original Draft, W.T.; Writing – Review & Editing, W.T. and C.M.; Supervision, C.M. and Z.W.

ACKNOWLEDGMENTS

We thank Y. Tomari for sharing unpublished data; S. Mitani for *parn-1 (tm869)* and *parn-2 (tm1339)* strains; J. Kim for the *henn-1 (tm4477)* mutant; E. Kittler and the University of Massachusetts Deep Sequencing Core for Illumina sequencing; M. Shirayama for his assistance with molecular cloning and generating *parn-1*; *parn-2* double mutants; W. Gu for bioinformatic analysis; D. Conte for comments on the text; and members of the Mello and Ambros labs and Y. Zhang for discussion. Some of the strains were provided by the Caenorhabditis Genetics Center. This work was supported in part by a Hope Funds for Cancer Research Postdoctoral fellowship to W. T.; an NIH Pathway to Independence Award (GM108866) to H.-C. L.; an NIH grant (HD078253) to Z.W.; and NIH grants (GM058800 and HD078253) to C.C.M. C.C.M. is a Howard Hughes Medical Institute Investigator.

Received: August 2, 2015
Revised: November 14, 2015
Accepted: February 3, 2016
Published: February 25, 2016

REFERENCES

Ashe, A., Sapetschnig, A., Weick, E.M., Mitchell, J., Bagijn, M.P., Cording, A.C., Doebley, A.L., Goldstein, L.D., Lehrbach, N.J., Le Pen, J., et al. (2012). piRNAs can trigger a multigenerational epigenetic memory in the germline of C. elegans. Cell *150*, 88–99.

Aström, J., Aström, A., and Virtanen, A. (1992). Properties of a HeLa cell 3′ exonuclease specific for degrading poly(A) tails of mammalian mRNA. J. Biol. Chem. *267*, 18154–18159.

Bagijn, M.P., Goldstein, L.D., Sapetschnig, A., Weick, E.M., Bouasker, S., Lehrbach, N.J., Simard, M.J., and Miska, E.A. (2012). Function, targets, and evolution of Caenorhabditis elegans piRNAs. Science *337*, 574–578.

Barberán-Soler, S., Fontrodona, L., Ribó, A., Lamm, A.T., Iannone, C., Cerón, J., Lehner, B., and Valcárcel, J. (2014). Co-option of the piRNA pathway for germline-specific alternative splicing of C. elegans TOR. Cell Rep. *8*, 1609–1616.

Bartel, D.P. (2009). MicroRNAs: target recognition and regulatory functions. Cell *136*, 215–233.

Batista, P.J., Ruby, J.G., Claycomb, J.M., Chiang, R., Fahlgren, N., Kasschau, K.D., Chaves, D.A., Gu, W., Vasale, J.J., Duan, S., et al. (2008). PRG-1 and 21U-RNAs interact to form the piRNA complex required for fertility in C. elegans. Mol. Cell *31*, 67–78.

Beanan, M.J., and Strome, S. (1992). Characterization of a germ-line proliferation mutation in C. elegans. Development *116*, 755–766.

Berndt, H., Harnisch, C., Rammelt, C., Stöhr, N., Zirkel, A., Dohm, J.C., Himmelbauer, H., Tavanez, J.P., Hüttelmaier, S., and Wahle, E. (2012). Maturation of mammalian H/ACA box snoRNAs: PAPD5-dependent adenylation and PARN-dependent trimming. RNA *18*, 958–972.

Billi, A.C., Alessi, A.F., Khivansara, V., Han, T., Freeberg, M., Mitani, S., and Kim, J.K. (2012). The Caenorhabditis elegans HEN1 ortholog, HENN-1, methylates and stabilizes select subclasses of germline small RNAs. PLoS Genet. *8*, e1002617.

Brawand, D., Soumillon, M., Necsulea, A., Julien, P., Csárdi, G., Harrigan, P., Weier, M., Liechti, A., Aximu-Petri, A., Kircher, M., et al. (2011). The evolution of gene expression levels in mammalian organs. Nature *478*, 343–348.

Brennecke, J., Stark, A., Russell, R.B., and Cohen, S.M. (2005). Principles of microRNA-target recognition. PLoS Biol. *3*, e85.

Brennecke, J., Aravin, A.A., Stark, A., Dus, M., Kellis, M., Sachidanandam, R., and Hannon, G.J. (2007). Discrete small RNA-generating loci as master regulators of transposon activity in Drosophila. Cell *128*, 1089–1103.

Brenner, S. (1974). The genetics of Caenorhabditis elegans. Genetics *77*, 71–94.

Carmell, M.A., Girard, A., van de Kant, H.J., Bourc'his, D., Bestor, T.H., de Rooij, D.G., and Hannon, G.J. (2007). MIWI2 is essential for spermatogenesis and repression of transposons in the mouse male germline. Dev. Cell *12*, 503–514.

Cecere, G., Zheng, G.X., Mansisidor, A.R., Klymko, K.E., and Grishok, A. (2012). Promoters recognized by forkhead proteins exist for individual 21U-RNAs. Mol. Cell *47*, 734–745.

Chen, C.C., Simard, M.J., Tabara, H., Brownell, D.R., McCollough, J.A., and Mello, C.C. (2005). A member of the polymerase beta nucleotidyltransferase superfamily is required for RNA interference in C. elegans. Curr. Biol. *15*, 378–383.

Conine, C.C., Moresco, J.J., Gu, W., Shirayama, M., Conte, D., Jr., Yates, J.R., 3rd, and Mello, C.C. (2013). Argonautes promote male fertility and provide a paternal memory of germline gene expression in C. elegans. Cell *155*, 1532–1544.

Conte, D., Jr., MacNeil, L.T., Walhout, A.J., and Mello, C.C. (2015). RNA Interference in Caenorhabditis elegans. Curr. Protoc. Mol. Biol. *109*, 1–30, 30.

Copeland, P.R., and Wormington, M. (2001). The mechanism and regulation of deadenylation: identification and characterization of Xenopus PARN. RNA *7*, 875–886.

Cox, D.N., Chao, A., Baker, J., Chang, L., Qiao, D., and Lin, H. (1998). A novel class of evolutionarily conserved genes defined by piwi are essential for stem cell self-renewal. Genes Dev. *12*, 3715–3727.

Das, P.P., Bagijn, M.P., Goldstein, L.D., Woolford, J.R., Lehrbach, N.J., Sapetschnig, A., Buhecha, H.R., Gilchrist, M.J., Howe, K.L., Stark, R., et al. (2008). Piwi and piRNAs act upstream of an endogenous siRNA pathway to suppress Tc3 transposon mobility in the Caenorhabditis elegans germline. Mol. Cell *31*, 79–90.

Deerberg, A., Willkomm, S., and Restle, T. (2013). Minimal mechanistic model of siRNA-dependent target RNA slicing by recombinant human Argonaute 2 protein. Proc. Natl. Acad. Sci. USA *110*, 17850–17855.

Feltzin, V.L., Khaladkar, M., Abe, M., Parisi, M., Hendriks, G.J., Kim, J., and Bonini, N.M. (2015). The exonuclease Nibbler regulates age-associated traits and modulates piRNA length in Drosophila. Aging Cell *14*, 443–452.

Friedman, R.C., Farh, K.K., Burge, C.B., and Bartel, D.P. (2009). Most mammalian mRNAs are conserved targets of microRNAs. Genome Res. *19*, 92–105.

Frøkjaer-Jensen, C., Davis, M.W., Hopkins, C.E., Newman, B.J., Thummel, J.M., Olesen, S.P., Grunnet, M., and Jorgensen, E.M. (2008). Single-copy insertion of transgenes in Caenorhabditis elegans. Nat. Genet. *40*, 1375–1383.

Goldstrohm, A.C., and Wickens, M. (2008). Multifunctional deadenylase complexes diversify mRNA control. Nat. Rev. Mol. Cell Biol. *9*, 337–344.

Gu, W., Shirayama, M., Conte, D., Jr., Vasale, J., Batista, P.J., Claycomb, J.M., Moresco, J.J., Youngman, E.M., Keys, J., Stoltz, M.J., et al. (2009). Distinct argonaute-mediated 22G-RNA pathways direct genome surveillance in the C. elegans germline. Mol. Cell *36*, 231–244.

Gu, W., Lee, H.C., Chaves, D., Youngman, E.M., Pazour, G.J., Conte, D., Jr., and Mello, C.C. (2012). CapSeq and CIP-TAP identify Pol II start sites and reveal capped small RNAs as C. elegans piRNA precursors. Cell *151*, 1488–1500.

Haley, B., and Zamore, P.D. (2004). Kinetic analysis of the RNAi enzyme complex. Nat. Struct. Mol. Biol. *11*, 599–606.

Han, B.W., Hung, J.H., Weng, Z., Zamore, P.D., and Ameres, S.L. (2011). The 3′-to-5′ exoribonuclease Nibbler shapes the 3′ ends of microRNAs bound to Drosophila Argonaute1. Curr. Biol. *21*, 1878–1887.

Han, B.W., Wang, W., Li, C., Weng, Z., and Zamore, P.D. (2015). Noncoding RNA. piRNA-guided transposon cleavage initiates Zucchini-dependent, phased piRNA production. Science *348*, 817–821.

Honda, S., Kirino, Y., Maragkakis, M., Alexiou, P., Ohtaki, A., Murali, R., Mourelatos, Z., and Kirino, Y. (2013). Mitochondrial protein BmPAPI modulates the length of mature piRNAs. RNA *19*, 1405–1418.

Horwich, M.D., Li, C., Matranga, C., Vagin, V., Farley, G., Wang, P., and Zamore, P.D. (2007). The Drosophila RNA methyltransferase, DmHen1, modifies germline piRNAs and single-stranded siRNAs in RISC. Curr. Biol. *17*, 1265–1272.

Houwing, S., Kamminga, L.M., Berezikov, E., Cronembold, D., Girard, A., van den Elst, H., Filippov, D.V., Blaser, H., Raz, E., Moens, C.B., et al. (2007). A role for Piwi and piRNAs in germ cell maintenance and transposon silencing in Zebrafish. Cell *129*, 69–82.

Ipsaro, J.J., Haase, A.D., Knott, S.R., Joshua-Tor, L., and Hannon, G.J. (2012). The structural biochemistry of Zucchini implicates it as a nuclease in piRNA biogenesis. Nature *491*, 279–283.

Ishizu, H., Siomi, H., and Siomi, M.C. (2012). Biology of PIWI-interacting RNAs: new insights into biogenesis and function inside and outside of germlines. Genes Dev. *26*, 2361–2373.

Izumi, N., Shoji, K., Sakaguchi, Y., Honda, S., Kirino, Y., Suzuki, T., Katsuma, S., and Tomari, Y. (2016). Identification and Functional Analysis of the Pre-piRNA 3′ Trimmer in Silkworms. Cell *164*, this issue, 962–973.

Kamminga, L.M., van Wolfswinkel, J.C., Luteijn, M.J., Kaaij, L.J., Bagijn, M.P., Sapetschnig, A., Miska, E.A., Berezikov, E., and Ketting, R.F. (2012). Differential impact of the HEN1 homolog HENN-1 on 21U and 26G RNAs in the germline of Caenorhabditis elegans. PLoS Genet. *8*, e1002702.

Kawaoka, S., Izumi, N., Katsuma, S., and Tomari, Y. (2011). 3′ end formation of PIWI-interacting RNAs in vitro. Mol. Cell *43*, 1015–1022.

Kawasaki, I., Shim, Y.H., Kirchner, J., Kaminker, J., Wood, W.B., and Strome, S. (1998). PGL-1, a predicted RNA-binding component of germ granules, is essential for fertility in C. elegans. Cell *94*, 635–645.

Ketting, R.F., Haverkamp, T.H., van Luenen, H.G., and Plasterk, R.H. (1999). Mut-7 of C. elegans, required for transposon silencing and RNA interference, is a homolog of Werner syndrome helicase and RNaseD. Cell *99*, 133–141.

Kirino, Y., and Mourelatos, Z. (2007). Mouse Piwi-interacting RNAs are 2′-O-methylated at their 3′ termini. Nat. Struct. Mol. Biol. *14*, 347–348.

Klattenhoff, C., and Theurkauf, W. (2008). Biogenesis and germline functions of piRNAs. Development *135*, 3–9.

Körner, C.G., and Wahle, E. (1997). Poly(A) tail shortening by a mammalian poly(A)-specific 3′-exoribonuclease. J. Biol. Chem. *272*, 10448–10456.

Körner, C.G., Wormington, M., Muckenthaler, M., Schneider, S., Dehlin, E., and Wahle, E. (1998). The deadenylating nuclease (DAN) is involved in poly(A) tail removal during the meiotic maturation of Xenopus oocytes. EMBO J. *17*, 5427–5437.

Lee, H.C., Gu, W., Shirayama, M., Youngman, E., Conte, D., Jr., and Mello, C.C. (2012a). C. elegans piRNAs mediate the genome-wide surveillance of germline transcripts. Cell *150*, 78–87.

Lee, J.E., Lee, J.Y., Trembly, J., Wilusz, J., Tian, B., and Wilusz, C.J. (2012b). The PARN deadenylase targets a discrete set of mRNAs for decay and regulates cell motility in mouse myoblasts. PLoS Genet. *8*, e1002901.

Li, X.Z., Roy, C.K., Dong, X., Bolcun-Filas, E., Wang, J., Han, B.W., Xu, J., Moore, M.J., Schimenti, J.C., Weng, Z., and Zamore, P.D. (2013). An ancient transcription factor initiates the burst of piRNA production during early meiosis in mouse testes. Mol. Cell *50*, 67–81.

Lin, H., and Spradling, A.C. (1997). A novel group of pumilio mutations affects the asymmetric division of germline stem cells in the Drosophila ovary. Development *124*, 2463–2476.

Liu, L., Qi, H., Wang, J., and Lin, H. (2011a). PAPI, a novel TUDOR-domain protein, complexes with AGO3, ME31B and TRAL in the nuage to silence transposition. Development *138*, 1863–1873.

Liu, N., Abe, M., Sabin, L.R., Hendriks, G.J., Naqvi, A.S., Yu, Z., Cherry, S., and Bonini, N.M. (2011b). The exoribonuclease Nibbler controls 3′ end processing of microRNAs in Drosophila. Curr. Biol. *21*, 1888–1893.

Luteijn, M.J., and Ketting, R.F. (2013). PIWI-interacting RNAs: from generation to transgenerational epigenetics. Nat. Rev. Genet. *14*, 523–534.

Malone, C.D., and Hannon, G.J. (2009). Small RNAs as guardians of the genome. Cell *136*, 656–668.

Malone, C.D., Brennecke, J., Dus, M., Stark, A., McCombie, W.R., Sachidanandam, R., and Hannon, G.J. (2009). Specialized piRNA pathways act in germline and somatic tissues of the Drosophila ovary. Cell *137*, 522–535.

Marasovic, M., Zocco, M., and Halic, M. (2013). Argonaute and Triman generate dicer-independent priRNAs and mature siRNAs to initiate heterochromatin formation. Mol. Cell *52*, 173–183.

Mohn, F., Handler, D., and Brennecke, J. (2015). Noncoding RNA. piRNA-guided slicing specifies transcripts for Zucchini-dependent, phased piRNA biogenesis. Science *348*, 812–817.

Montgomery, T.A., Rim, Y.S., Zhang, C., Dowen, R.H., Phillips, C.M., Fischer, S.E., and Ruvkun, G. (2012). PIWI associated siRNAs and piRNAs specifically require the Caenorhabditis elegans HEN1 ortholog henn-1. PLoS Genet. *8*, e1002616.

Nishimasu, H., Ishizu, H., Saito, K., Fukuhara, S., Kamatani, M.K., Bonnefond, L., Matsumoto, N., Nishizawa, T., Nakanaga, K., Aoki, J., et al. (2012). Structure and function of Zucchini endoribonuclease in piRNA biogenesis. Nature *491*, 284–287.

Nousch, M., Techritz, N., Hampel, D., Millonigg, S., and Eckmann, C.R. (2013). The Ccr4-Not deadenylase complex constitutes the main poly(A) removal activity in C. elegans. J. Cell Sci. *126*, 4274–4285.

Olivieri, D., Sykora, M.M., Sachidanandam, R., Mechtler, K., and Brennecke, J. (2010). An in vivo RNAi assay identifies major genetic and cellular requirements for primary piRNA biogenesis in Drosophila. EMBO J. *29*, 3301–3317.

Pane, A., Wehr, K., and Schüpbach, T. (2007). zucchini and squash encode two putative nucleases required for rasiRNA production in the Drosophila germline. Dev. Cell *12*, 851–862.

Petryszak, R., Burdett, T., Fiorelli, B., Fonseca, N.A., Gonzalez-Porta, M., Hastings, E., Huber, W., Jupp, S., Keays, M., Kryvych, N., et al. (2014). Expression Atlas update–a database of gene and transcript expression from microarray- and sequencing-based functional genomics experiments. Nucleic Acids Res. *42*, D926–D932.

Ren, Y.G., Kirsebom, L.A., and Virtanen, A. (2004). Coordination of divalent metal ions in the active site of poly(A)-specific ribonuclease. J. Biol. Chem. *279*, 48702–48706.

Ruby, J.G., Jan, C., Player, C., Axtell, M.J., Lee, W., Nusbaum, C., Ge, H., and Bartel, D.P. (2006). Large-scale sequencing reveals 21U-RNAs and additional microRNAs and endogenous siRNAs in C. elegans. Cell *127*, 1193–1207.

Saito, K., Sakaguchi, Y., Suzuki, T., Suzuki, T., Siomi, H., and Siomi, M.C. (2007). Pimet, the Drosophila homolog of HEN1, mediates 2′-O-methylation of Piwi- interacting RNAs at their 3′ ends. Genes Dev. *21*, 1603–1608.

Salomon, W.E., Jolly, S.M., Moore, M.J., Zamore, P.D., and Serebrov, V. (2015). Single-Molecule Imaging Reveals that Argonaute Reshapes the Binding Properties of Its Nucleic Acid Guides. Cell *162*, 84–95.

Saxe, J.P., Chen, M., Zhao, H., and Lin, H. (2013). Tdrkh is essential for spermatogenesis and participates in primary piRNA biogenesis in the germline. EMBO J. *32*, 1869–1885.

Senti, K.A., and Brennecke, J. (2010). The piRNA pathway: a fly's perspective on the guardian of the genome. Trends Genet. *26*, 499–509.

Seth, M., Shirayama, M., Gu, W., Ishidate, T., Conte, D., Jr., and Mello, C.C. (2013). The C. elegans CSR-1 argonaute pathway counteracts epigenetic silencing to promote germline gene expression. Dev. Cell *27*, 656–663.

Shirayama, M., Seth, M., Lee, H.C., Gu, W., Ishidate, T., Conte, D., Jr., and Mello, C.C. (2012). piRNAs initiate an epigenetic memory of nonself RNA in the C. elegans germline. Cell *150*, 65–77.

Simon, B., Kirkpatrick, J.P., Eckhardt, S., Reuter, M., Rocha, E.A., Andrade-Navarro, M.A., Sehr, P., Pillai, R.S., and Carlomagno, T. (2011). Recognition of 2′-O-methylated 3′-end of piRNA by the PAZ domain of a Piwi protein. Structure *19*, 172–180.

Simon, M., Sarkies, P., Ikegami, K., Doebley, A.L., Goldstein, L.D., Mitchell, J., Sakaguchi, A., Miska, E.A., and Ahmed, S. (2014). Reduced insulin/IGF-1 signaling restores germ cell immortality to Caenorhabditis elegans Piwi mutants. Cell Rep. *7*, 762–773.

Siomi, M.C., Sato, K., Pezic, D., and Aravin, A.A. (2011). PIWI-interacting small RNAs: the vanguard of genome defence. Nat. Rev. Mol. Cell Biol. *12*, 246–258.

Tabara, H., Sarkissian, M., Kelly, W.G., Fleenor, J., Grishok, A., Timmons, L., Fire, A., and Mello, C.C. (1999). The rde-1 gene, RNA interference, and transposon silencing in C. elegans. Cell *99*, 123–132.

Tian, Y., Simanshu, D.K., Ma, J.B., and Patel, D.J. (2011). Structural basis for piRNA 2′-O-methylated 3′-end recognition by Piwi PAZ (Piwi/Argonaute/Zwille) domains. Proc. Natl. Acad. Sci. USA *108*, 903–910.

van der Heijden, G.W., Castañeda, J., and Bortvin, A. (2010). Bodies of evidence - compartmentalization of the piRNA pathway in mouse fetal prospermatogonia. Curr. Opin. Cell Biol. *22*, 752–757.

Vourekas, A., Zheng, Q., Alexiou, P., Maragkakis, M., Kirino, Y., Gregory, B.D., and Mourelatos, Z. (2012). Mili and Miwi target RNA repertoire reveals piRNA biogenesis and function of Miwi in spermiogenesis. Nat. Struct. Mol. Biol. *19*, 773–781.

Wang, G., and Reinke, V. (2008). A C. elegans Piwi, PRG-1, regulates 21U-RNAs during spermatogenesis. Curr. Biol. *18*, 861–867.

Wedeles, C.J., Wu, M.Z., and Claycomb, J.M. (2013). Protection of germline gene expression by the C. elegans Argonaute CSR-1. Dev. Cell *27*, 664–671.

Weick, E.M., and Miska, E.A. (2014). piRNAs: from biogenesis to function. Development *141*, 3458–3471.

Weick, E.M., Sarkies, P., Silva, N., Chen, R.A., Moss, S.M., Cording, A.C., Ahringer, J., Martinez-Perez, E., and Miska, E.A. (2014). PRDE-1 is a nuclear factor essential for the biogenesis of Ruby motif-dependent piRNAs in C. elegans. Genes Dev. *28*, 783–796.

Yoda, M., Cifuentes, D., Izumi, N., Sakaguchi, Y., Suzuki, T., Giraldez, A.J., and Tomari, Y. (2013). Poly(A)-specific ribonuclease mediates 3′-end trimming of Argonaute2-cleaved precursor microRNAs. Cell Rep. *5*, 715–726.

Zuo, Y., and Deutscher, M.P. (2001). Exoribonuclease superfamilies: structural analysis and phylogenetic distribution. Nucleic Acids Res. *29*, 1017–1026.